Analytical modeling of the input admittance of an electric drive for stability analysis purposes

Sylvain Girinon, Cédric Baumann, Hubert Piquet, Nicolas Roux

EPJ manuscript No.
(will be inserted by the editor)

Analytical modeling of the input admittance of an electric drive for stability analysis purposes

S. Girinon[1], C. Baumann[2], H. Piquet[1], and N. Roux[1]

[1] Université de Toulouse, LAboratoire PLAsma et Conversion d'Energie *(LAPLACE)*, CNRS *(UMR 5213)*, INPT, UPS, 2 rue Camichel, BP 7122, 31071 Toulouse Cedex 7, France
[2] AIRBUS France S.A.S., 316 Route de Narbonne P.O. BOX M0131/5, 31060 Toulouse Cedex 9, FRANCE

Received: date / Revised version: date

Abstract. Embedded electric HVDC distribution network are facing difficult issues on quality and stability concerns. In order to help to resolve those problems, this paper proposes to develop an analytical model of an electric drive. This self-contained model includes an inverter, its regulation loops and the PMSM. After comparing the model with its equivalent (abc) full model, the study focuses on frequency analysis. The association with an input filter helps in expressing stability of the whole assembly by means of Routh-Hurtwitz criterion.

1 Introduction

In the electrical distribution context, this paper deals with the design specification of HVDC embedded network. More precisely, filters between distribution network and power electronics loads have to be chosen properly in order to minimize weight and size in a constrained environment.

The purpose is to develop an input admittance model of an electric drive. Voltage inverter, its control loops and the PMSM associated with its mechanical load are considered. Model will be used in order to study stability and quality performances of this equipment. Preceding studies consist mainly in comparing input load and output source impedance based on Middlebrook criterion [1], [2].

Once established the time-domain analytical nonlinear model of the whole system in the Park frame, we propose significant simulation results obtained with the *Saber* simulator. They validate the model accuracy, in transient as well as in steady state conditions. The proposed model is compared to a full (abc) one, taking into account the switchings in the inverter.

A frequency-domain analytical model of the equipment is then derived, by mean of linearization around a given operating point. Comparison of the Bode plots of both time-domain and frequency-domain models establishes the accuracy of the latter. It is then associated with its input filter and used for stability analyzes: the *Routh-Hurwitz* criterion is applied to the symbolic expressions of the transfer function in order to predict the stability of the whole assembly, considering the effect of the stiffness of the control loops and the input filter design. Time domain simulations of some chosen cases validate the predicted stability properties.

November 01, 2007

2 The system under study

The system under study is given in (Fig. 1). A three-phase variable frequency generator (typically 360Hz<f<800Hz) supplies a DC bus through a rectifier. A filter is connected between the load and the bus.

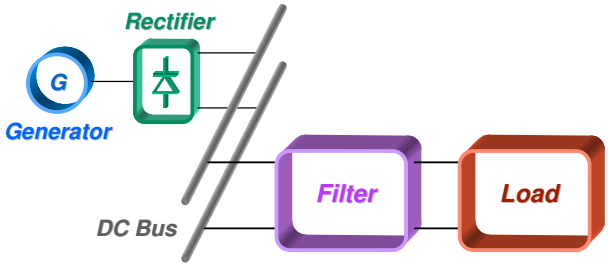

Fig. 1. The studied system

The system consists of three separable parts, which are the supply, the filter and the load. The supply part includes the generator and the rectifier which delivers the electrical power to the DC bus. First, the model of the supply is presented.

The supply is modeled with an equivalent DC voltage source (V_e) in series with an inductor (L_{supply}) and a re-

sistor (R_{supply}). The wires are modeled by the resistor: ohmic characteristic, skin and proximity effects [3]. It also figures the overlapping introduced by the rectifier [4].

If the AC/DC stage of the supply includes an auto-transformer unit, its actual characteristics are also taken into account with the R_{supply} and L_{supply} components.

Nevertheless, for this first stability study, the worst case will be considered neglecting the damping effect of R_{supply}.

3 Time domain modeling of the drive

A representation of the system and the variables associated to the drive is given in (Figure 2).

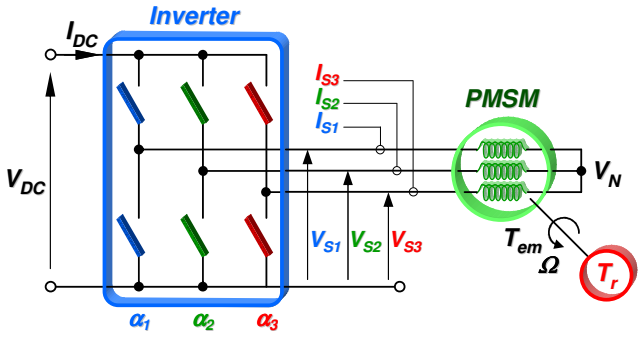

Fig. 2. Presentation of the complete load

The whole system is studied in a Park frame and the d axis of which is associated to the rotor magnet. A description of each part is discussed in the following sub-sections. The objective is to obtain an admittance describing the behaviour of the inverter associated with the PMSM, connected to the DC bus. The mechanical part consists in a rotational shaft as described in figure (3). The control loops will be introduced in a second step; they will define the values of the I_d^{ref} and I_q^{ref} quantities.

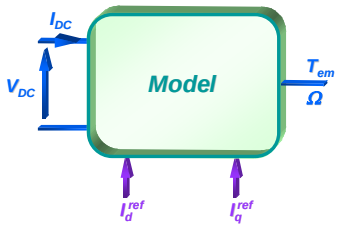

Fig. 3. Model representation

3.1 PMSM modeling

The behaviour of the mechanical part of the system is stated in (1).

$$J\frac{d\Omega(t)}{dt} + f\Omega(t) = T_{em} - T_r \tag{1}$$

... where J is the moment of inertia of the machine. f is the friction coefficient and Ω the rotation speed. T_{em} represents the electromechanical torque and T_r the load torque.

The Park frame is used in (2) and (3) in order to model the electrical part.

$$\begin{cases} V_d(t) = R_s I_d(t) + L_d\dfrac{dI_d(t)}{dt} + e_d(t) \\ V_q(t) = R_s I_q(t) + L_q\dfrac{dI_q(t)}{dt} + e_q(t) \end{cases} \tag{2}$$

$$\begin{cases} e_d(t) = -\omega_s L_q I_q(t) \\ e_q(t) = \omega_s(L_d I_d(t) + \phi_M) \end{cases} \tag{3}$$

... where V_d and V_q are the stator voltages in the Park frame, R_s the stator resistor, L_d and L_q the stator inductors, I_d and I_q are the stator currents in the Park frame and ϕ_M is the no-load flux. ω_s is the electrical stator pulse, so $\omega_s = N_p\Omega$.

The general torque expression is given in (4).

$$T_{em}(t) = \sqrt{\frac{3}{2}}N_p(\psi_d(t)I_q(t) - \psi_q(t)I_d(t)) \tag{4}$$

... where N_p is the number of pole pairs and ψ_d and ψ_q are defined in (5).

$$\begin{cases} \psi_d(t) = L_d I_d + \phi_M \\ \psi_q(t) = L_q I_q \end{cases} \tag{5}$$

3.2 Inverter modeling

As the neutral point of the machine is not connected to the ground, (6) gives its voltage, assuming that the PMSM is balanced.

$$V_N = \frac{1}{3}(V_{s1} + V_{s2} + V_{s3}) \tag{6}$$

Considering the inverter operation, stator voltages are expressed in relation with the DC voltage (V_{DC}) as in (7).

$$\begin{pmatrix} V_{s1} \\ V_{s2} \\ V_{s3} \end{pmatrix} = V_{DC}\begin{pmatrix} \alpha_1 \\ \alpha_2 \\ \alpha_3 \end{pmatrix} \tag{7}$$

... where α_i are the duty cycle on each inverter leg.

Finally, we apply the Park transformation $[P]$ to the stator voltages, which leads to (8).

$$\begin{pmatrix} V_d \\ V_q \\ V_h \end{pmatrix} = [P] \begin{pmatrix} V_{s1} \\ V_{s2} \\ V_{s2} \end{pmatrix} - [P] \begin{pmatrix} V_N \\ V_N \\ V_N \end{pmatrix} \tag{8}$$

Introducing (6), we obtain (9) :

$$\begin{pmatrix} V_d \\ V_q \\ V_h \end{pmatrix} = \frac{V_{DC}}{3} [P] \begin{pmatrix} 2 & -1 & -1 \\ -1 & 2 & -1 \\ -1 & -1 & 2 \end{pmatrix} \begin{pmatrix} \alpha_1 \\ \alpha_2 \\ \alpha_3 \end{pmatrix} \tag{9}$$

We consider a power conservative to define three duty cycles in the Park frame (α_d, α_q, α_h). Those duty cycles permit an use of the inverter similar to the classical one in the (abc) frame (7). Output voltages in the Park frame are defined in (10).

$$\begin{pmatrix} V_d \\ V_q \\ V_h \end{pmatrix} = \begin{pmatrix} \alpha_d \\ \alpha_q \\ \alpha_h \end{pmatrix} V_{DC} \tag{10}$$

The neutral point being disconnected from the ground, it is possible to analytically express the Park duty cycles (11).

$$\begin{aligned} \begin{pmatrix} \alpha_d \\ \alpha_q \\ \alpha_h \end{pmatrix} &= \frac{1}{3}[P] \begin{pmatrix} 2 & -1 & -1 \\ -1 & 2 & -1 \\ -1 & -1 & 2 \end{pmatrix} \begin{pmatrix} \alpha_1 \\ \alpha_2 \\ \alpha_3 \end{pmatrix} \\ &= \begin{pmatrix} \gamma_{11} & \gamma_{12} & \gamma_{13} \\ \gamma_{21} & \gamma_{22} & \gamma_{23} \\ 0 & 0 & 0 \end{pmatrix} \begin{pmatrix} \alpha_1 \\ \alpha_2 \\ \alpha_3 \end{pmatrix} \end{aligned} \tag{11}$$

$$\begin{aligned} \gamma_{11} &= \frac{2}{\sqrt{6}} cos(\theta) \\ \gamma_{12} &= -\frac{1}{\sqrt{6}} cos(\theta) + \frac{1}{\sqrt{2}} sin(\theta) \\ \gamma_{13} &= -\frac{1}{\sqrt{6}} cos(\theta) - \frac{1}{\sqrt{2}} sin(\theta) \\ \gamma_{21} &= -\frac{2}{\sqrt{6}} sin(\theta) \\ \gamma_{22} &= \frac{1}{\sqrt{2}} cos(\theta) + \frac{1}{\sqrt{6}} sin(\theta) \\ \gamma_{23} &= -\frac{1}{\sqrt{2}} cos(\theta) + \frac{1}{\sqrt{6}} sin(\theta) \end{aligned}$$

As $\alpha_h = 0$, a total control of the load in the Park frame needs only controlling I_d and I_q.

The final step of the inverter modeling consists in the determination of the DC current expression which depends on the load. This is important in order to have the load behaviour according to the DC bus voltage.

Considering a perfect inverter - without losses - the entire power is transferred from DC side to AC side as expressed in (12).

$$P_{inv}|_{in} = P_{inv}|_{out} \Longrightarrow V_{DC} I_{DC} = \sum_{k=1}^{3} V_{sk} I_{sk} \tag{12}$$

As the chosen Park transformation is power conservative, a similar expression may be written:

$$\sum_{k=1}^{3} V_{sk} I_{sk} = \sum_{k=d,q,h} V_k I_k \tag{13}$$

Finally, considering (10) and $\alpha_h = 0$, the DC current is expressed:

$$I_{DC} = \begin{pmatrix} \alpha_d & \alpha_q \end{pmatrix} \begin{pmatrix} I_d \\ I_q \end{pmatrix} \tag{14}$$

4 Load control

The control apparatus of the drive regulates both currents in (d,q) axis. PI regulators - including anti-windup systems and electromotive force compensation - are designed. A representation of the control part is given in figure (4).

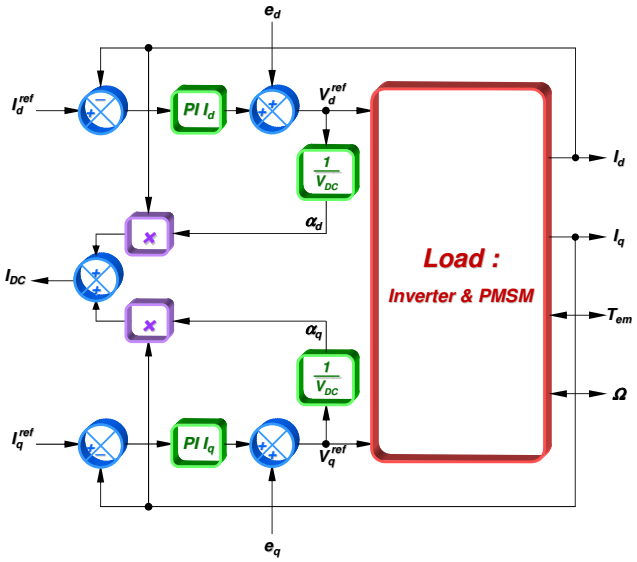

Fig. 4. Control part

5 Model validation comparing simulations results between our model and an (a,b,c) one

In order to establish the validity of the simulation results of the Park model, $I_q^{ref} = 97.62A$ and $I_d^{ref} = 0A$ are imposed. PMSM torque being controlled, the PMSM starting is realized applying a step on I_q^{ref}, in order to produce the rated torque. No control loop for drive speed has been implemented. Those choices help to determine the operating point as a simple mechanical load is connected to the shaft. The mechanical load has a viscous damping effect with a friction coefficient (f_{load}) corresponding to a nominal speed delivered with a nominal torque reference.

Each simulation result is obtained by two different means:

- a full reference model using a behavioral model of the PMSM and taking into account the inverter switching
- our model, fully implemented in the (dq) axis for both the inverter and the PMSM

Studied machine is a surface mounted permanent-magnet machine, hence $L_d = L_q = L_{dq}$. Moreover, a table containing parameters values of studied system is proposed in appendix.

The first figure presenting simulation results (Fig. 5) shows a validation of the mechanical operation of the load.

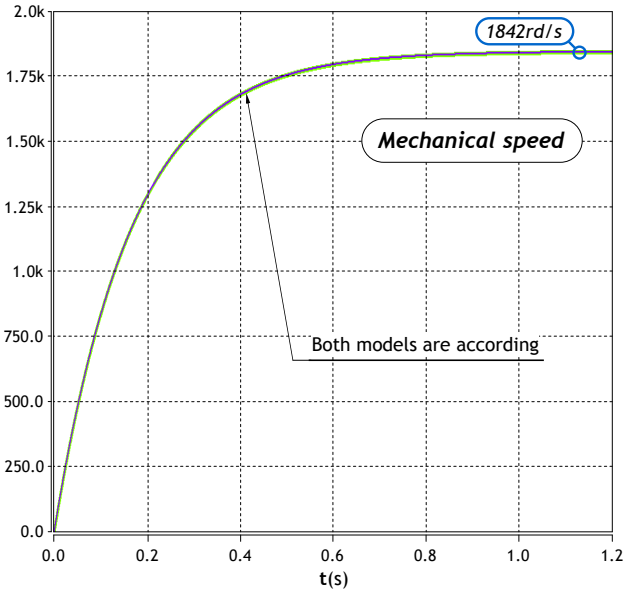

Fig. 5. Mechanical speed with a torque control. The two curves are layered

The system is starting from 0 to $\Omega = 1842 rad.s^{-1}$, which corresponds to the steady state speed regarding the conditions (15).

$$\Omega(\infty) = \frac{T_{em}}{f + f_{load}} \tag{15}$$

As an illustration of the model validation, (Fig. 6) demonstrates that (q) axis current is the same in both simulations.

Finally, in order to validate the model regarding DC connections, (Fig. 7) shows DC current absorbed by the system. The current supplied by the generator in the full model has been filtered in order to directly compare it with the other one.

As a conclusion, the Park model of the entire system is relevant as the simulation results match the different characteristics of (abc) full model. Note that the computation times change with the used model. In fact, to simulate $100ms$ with the same CPU and with the same simulation

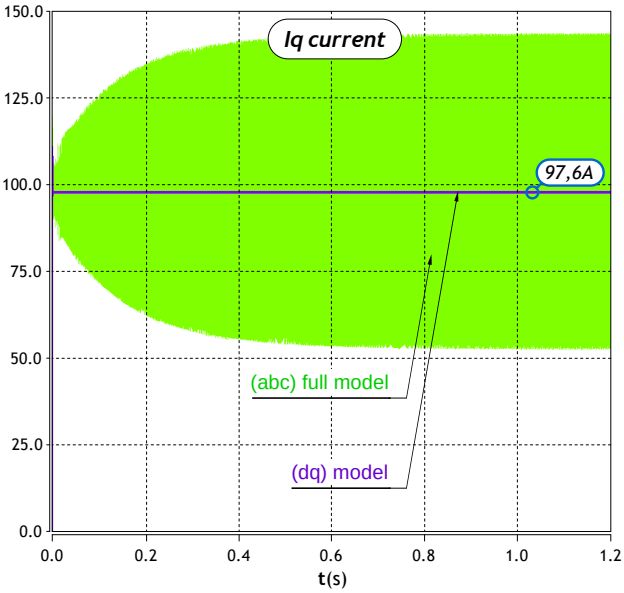

Fig. 6. Current regulation on q axis

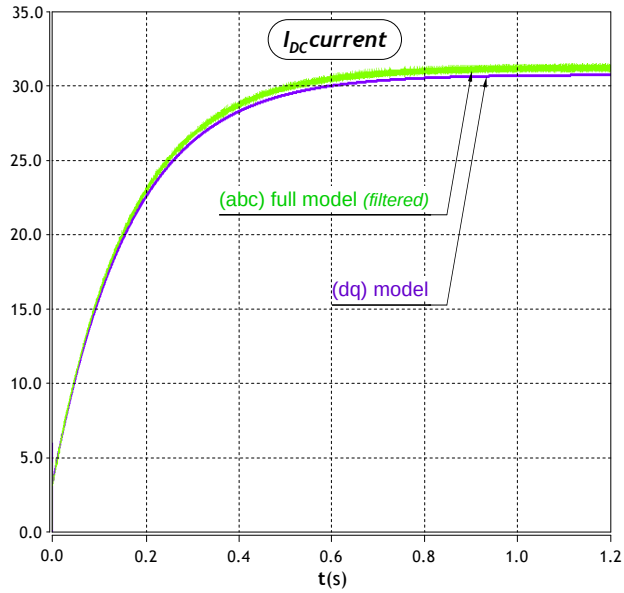

Fig. 7. Currents supplied by the DC source

software, the full model needs approximatively $500s$ and the (dq) model only needs less than $1s$.

6 Frequency domain modeling

In this section, the purpose is to model the drive by an equivalent admittance, described in the frequency domain. This way of modeling is also used in [5] and [2]. A library will be able to be built for several loads. With it, the study presented in part (7) can be generalized for various applications.

To reach a frequency model, the Laplace transform is applied to the expressions defined in (2) to obtain (16).

The mechanical speed is supposed constant because the rotor inertia is high. So the mechanical time constant is higher than the electrical one. Consequently, the speed variation has no influence on the current response.

$$\begin{cases} I_d(s) = \dfrac{1}{R_s + L_d \cdot s}(V_d + N_p \Omega L_q I_q) \\ I_q(s) = \dfrac{1}{R_s + L_q \cdot s}\left(V_q - N_p \Omega (L_d I_d + \phi_M)\right) \end{cases} \tag{16}$$

These expressions describe the operation of the PMSM. Then, the inverter is added with its regulation and compensation loops to obtain the block diagram presented in (Fig. 8). Note that the control loops consist of integral proportional regulators on each current.

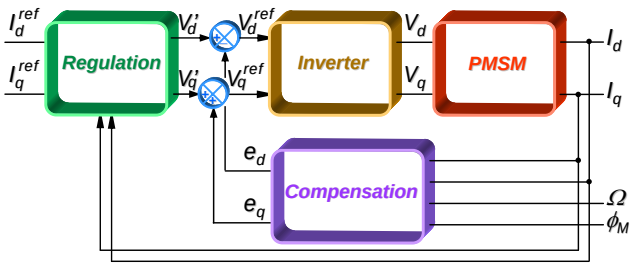

Fig. 8. Block diagram representing the system

The model uses power balance between the input and the output of the inverter defined in (12). The system is non-linear; therefore a linearization is necessary. As in [6], an averaged model linearized around an operating point will be considered. Considering X_0 as the operating point and δx as the variation of the variable X around X_0, equation (12) becomes (17).

$$\begin{aligned} \delta v_{DC} \cdot I_{DC0} + V_{DC0} \cdot \delta i_{DC} = \delta v_d \cdot I_{d0} + V_{d0} \cdot \delta i_d + \dots \\ \dots + \delta v_q \cdot I_{q0} + V_{q0} \cdot \delta i_q \end{aligned} \tag{17}$$

The following expressions of voltages in Park frame (18) are gathered from the block diagram (Fig. 8).

$$\begin{cases} V_d(s) = G \cdot V_{DC}\left(V_d' - N_p \Omega L_q I_q\right) \\ V_q(s) = G \cdot V_{DC}\left(V_q' + N_p \Omega \left(L_d I_d + \phi_M\right)\right) \end{cases} \tag{18}$$

... where G *is an adaptive gain in the inverter model. Note that L_d and L_q have been considered separately in order to keep a general expression, regardless the kind of PMSM. The model expression will be simplified afterwards so as to adapt to the chosen motor.*

The gain G used in (18) allows to take into account the variations of the DC voltage V_{DC} which supplies the inverter. As this voltage may differ from its nominal V_{DC0} value, the actual voltages (V_d, V_q) at the output of the inverter will not match exactly their references $(V_{d_{ref}}, V_{q_{ref}})$. Thus $G = \frac{1}{V_{DC0}}$ is introduced.

Equations (19) are a linearized form of (18).

$$\begin{cases} \delta v_d(s) = & G \cdot V_{DC0}\left(\delta v_d' - N_p \Omega L_q \delta i_q\right) \\ & + G \cdot \left(V_{d0}' - N_p \Omega L_q I_{q0}\right) \delta v_{DC} \\ \delta v_q(s) = & G \cdot V_{DC0}\left(\delta v_q' - N_p \Omega L_d \delta i_d\right) \\ & + G \cdot \left(V_{q0}' - N_p \Omega \left(L_d I_{d0} + \phi_M\right)\right) \delta v_{DC} \end{cases} \tag{19}$$

Substituting (19) in (17) gives the expression of the admittance Y (20).

$$Y(s) = \frac{\delta i_{DC}(s)}{\delta v_{DC}(s)} = \frac{\alpha_0 + \alpha_1 s + \alpha_2 s^2}{\beta_0 + \beta_1 s + \beta_2 s^2} \tag{20}$$

With:

$$\begin{aligned} \alpha_0 = & -G K_p V_{DC0} I_{DC0} \\ \alpha_1 = & \ \tau_i \Big[G R_s I_{q0} (V_{q0}' + N_p \Omega \phi_M) + G^2 V_{DC0} V_{q0}'^2 \\ & - I_{DC0}(G K_p V_{DC0} + R_s) + G^2 V_{DC0} N_p \Omega \\ & \phi_M (2 V_{q0}' + N_p \Omega \phi_M) \Big] \\ \alpha_2 = & \ \tau_i L_{dq} \Big[G V_{q0}' I_{q0} + G N_p \Omega I_{q0} \phi_M - I_{DC0} \Big] \\ \beta_0 = & \ G K_p V_{DC0}^2 \\ \beta_1 = & \ \tau_i (G K_p V_{DC0} + R_s) V_{DC0} \\ \beta_2 = & \ \tau_i L_{dq} V_{DC0} \end{aligned}$$

... where K_p and τ_i are, respectively, the proportional and the integral coefficients of current loops regulators.

This expression depends on the physical parameters of the machine (R_s, L_{dq}, N_p and ϕ_M), the regulator parameters (K_p and τ_i) and the chosen operating point. This operating point can be analytically specified.

In fact, currents I_{d0} and I_{q0} are given by the vectorial control of the PMSM [7]. Assuming that the (dq) axes angle (θ_{dq}) is equal to the electrical rotor angle (θ_r), currents are given by (21).

$$\begin{cases} I_{d0} = 0 \\ I_{q0} = \sqrt{\dfrac{2}{3}} \dfrac{T_{em}}{N_p \cdot \phi_M} \end{cases} \tag{21}$$

Voltages V_{d0} and V_{q0} are obtained with a vectorial representation. Thus, voltages V_{d0}' and V_{q0}' are obtained through a substitution of the compensation terms (22).

$$\begin{cases} V'_{d0} = -L_{dq}\cdot\omega_s\cdot I_{q0} + N_p\cdot\Omega\cdot L_{dq}\cdot I_{q0} = 0 \\ V'_{q0} = E + R_s\cdot I_{q0} - N_p\cdot\Omega\cdot\phi_M = R_s\cdot I_{q0} \end{cases} \quad (22)$$

... where E *is the electromotive force. Simplification is made knowing that:* $E = N_p\cdot\Omega\cdot\phi_M$.

Furthermore, the regulator parameters are calculated according to the wished performances (bandwidth and damping coefficient) using an abacus. The electrical part of the system with the current control loop can be approximated as a second-order model (*association of two first-order system*). Comparing this model with the canonical form of a second-order model, expressions (23) are obtained.

$$\begin{cases} K_p = 2\xi\cdot L_{dq}\cdot\omega_0 - R_s \\ \tau_i = \dfrac{2\xi}{\omega_0} - \dfrac{R_s}{L_{dq}\cdot\omega_0^2} \end{cases} \quad (23)$$

... where ω_0 *(natural frequency, an image of bandwidth) and* ξ *(damping coefficient) represent the wished parameters introduced in the canonical form.*

A simulation is performed with *Saber* to validate this model. The Bode diagram (Fig. 9) is plotted with solid lines for the model and with round points for the simulation results.

To conclude, the model well reproduces the frequency behaviour of the system in this range of frequency. It is not necessary to check the model reliability for higher frequencies. In fact, it concerns an average model, usable for frequencies below the switching frequency (20kHz in this example).

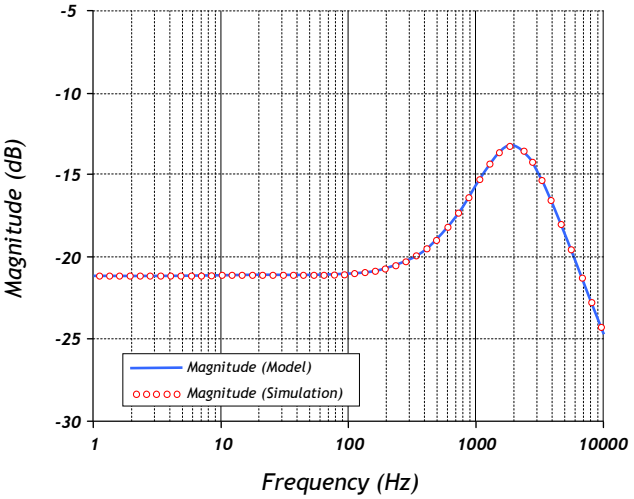

(a) Magnitude of the admittance Y

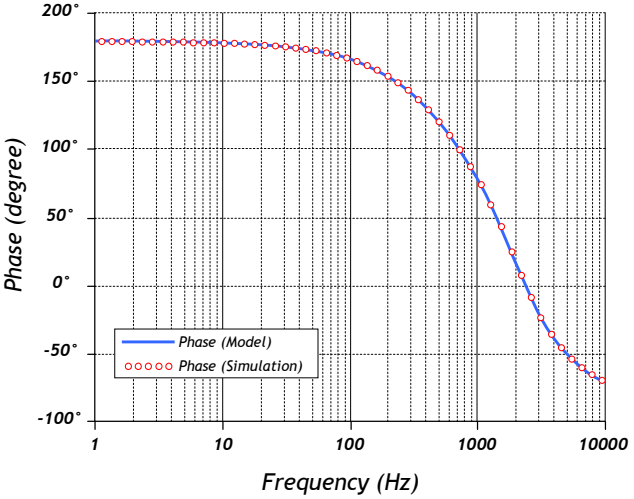

(b) Phase of the admittance Y

Fig. 9. Bode diagram of the admittance Y

7 Stability studies

The system that will be used for this study is reminded in (Fig. 10).

The filter consists of two cells, to eliminate high and low frequencies. The first filter cell allows to remove low frequencies on the DC side. Moreover, a resistor is used to reduce the resonance effect. Finally, the second filter cell allows removing the switching harmonics.

It is composed of two inductors *(currents are state variables)* and two capacitors *(voltages are state variables)*, therefore it will be a 4TH order system. Note that the power supply (L_{supply}) and filter (L_0) inductors are merged in the considered system.

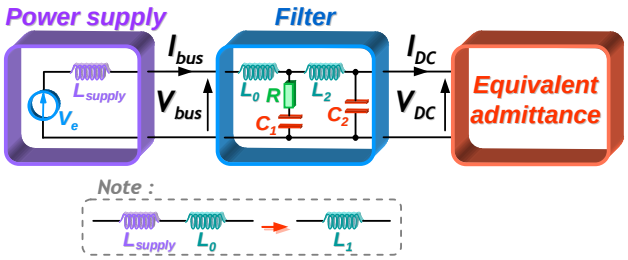

Fig. 10. The studied system

The different steps of the study are presented in (Fig. 11). First, the transfer function including the supply, the filter and the equivalent admittance is automatically determined with *Maple*. A tool has been developed, using a package called *Syrup*, to extract a symbolic model of the system from a netlist.

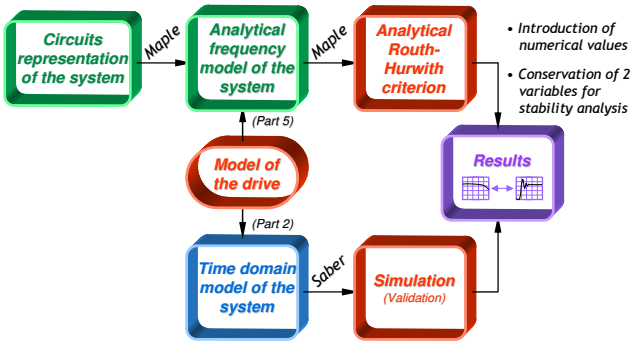

Fig. 11. The progress of the study

Then, stability analysis are performed on the model and results are validated by simulation.

For this application, a *6TH* order denominator is obtained (24), corresponding to the association of the filter *(4TH order)* and the load *(2TH order)*.

$$D(s) = \alpha_6 s^6 + \alpha_5 s^5 + \alpha_4 s^4 + \alpha_3 s^3 + \alpha_2 s^2 + \ldots \\ \ldots + \alpha_1 s + \alpha_0 \quad (24)$$

Studies are difficult due to the important number of parameters in several coefficients α_i. The *Routh-Hurwith* criterion appears as the most appropriated tool to study the stability. To carry out analysis, numerical values are introduced and we focus on two chosen parameters.

For a defined drive, at the chosen operating point, it is interesting to study the influence of the filter and regulation loops parameters. These parts are designed to fulfill requirements. Indeed, the filter, is designed to limit the current and voltage ripples; and the regulation loops, to ensure performances. Thus, it is useful to have an image of the system stability on range of values for those parameters. The following parts present studies which are performed on those domains.

7.1 Study on the filter parameters

On the one hand, the studies are performed on the filter parameters. Commonly, the filter size is wished as small as possible. So, the calculations will be carried out on the inductive and capacitive elements. For both parameters, L_1 and C_2, a sweep in a range of values is applied. The results are presented in (Figure 12).

In this figure, two areas appear separated by the stability limit. The red (dark) area represents the combinations of parameters leading to an unstable response, and consequently, the second area is the stable area.

Time domain simulations for two particular points are performed to check those results. According to the figure 10, the supply and the filter are added to the *dq Model*

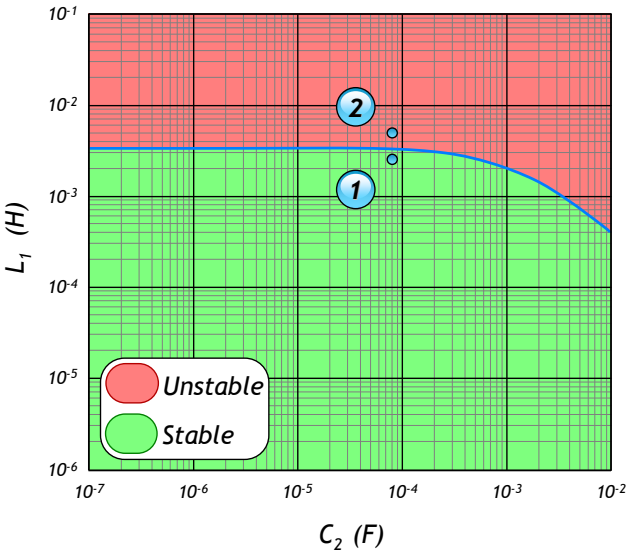

Fig. 12. Stability analysis with a sweep on $\{L_1, C_2\}$ parameters

developed and used in the part (5). The complete system is then simulated with *Saber* and results are presented in (Fig. 13).

First, the steady state is obtained with specific filter values ($L_1 = 20\mu H$, $C_2 = 80\mu F$). Then, a step is applied on rectified generator voltage (V_e) (in view of the fact that model is the transfer function between V_{DC} and V_e) from 540 to 550 volts. L_1 and C_2 values are then changed in accordance with the studied point on abacus.

Theses curves represent the voltage evolution across the load. Note that the voltage step on the bus is applied after $0,1s$.

- Figure 13(a) presents voltage across the drive with the filter values defined at the point 1, in the stable area. Voltage converges to the operating point in agreement with figure 12.
- Figure 13(b) presents the same voltage with filter values defined at the point 2, in the unstable area. Here, voltage diverges as expected according to figure 12.

In conclusion for this first part, simulation results agree with the analysis results given by the *Routh-Hurwith* criterion. To reach a stable system, the designer can take parameter combinations which belong to the stable area.

7.2 Study on the regulation parameters

On the other hand, the studies will be performed on the regulator parameters. As the dynamics influences stability margins, computations are now carried out on K_p (23) and filter resistor R (Fig. 10) parameters. The results are presented in (Figure 14).

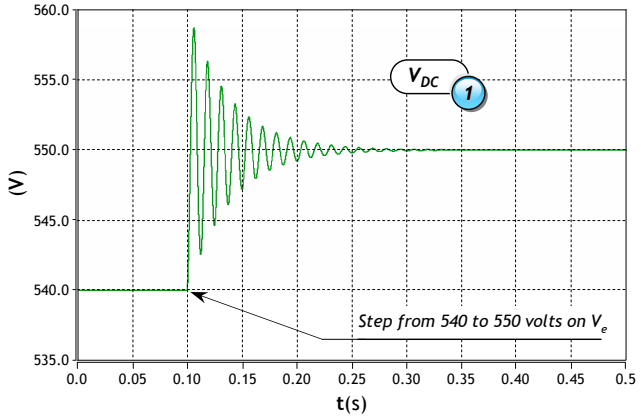

(a) Simulation with the parameters defined in point 1 ($L_1 = 2,5mH$ and $C_2 = 80\mu F$)

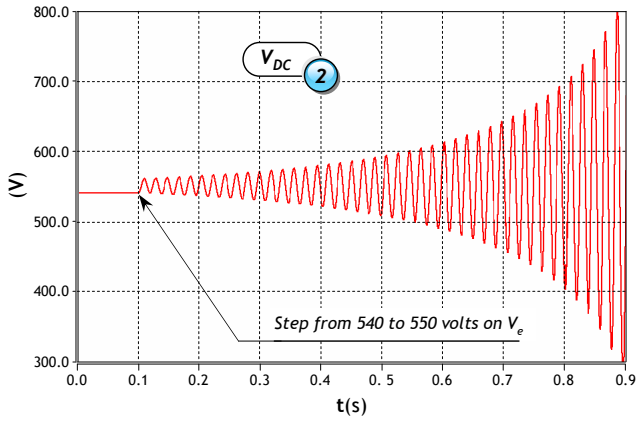

(b) Simulation with the parameters defined in point 2 ($L_1 = 5mH$ and $C_2 = 80\mu F$)

Fig. 13. V_{DC} voltage evolution for different L_1 values

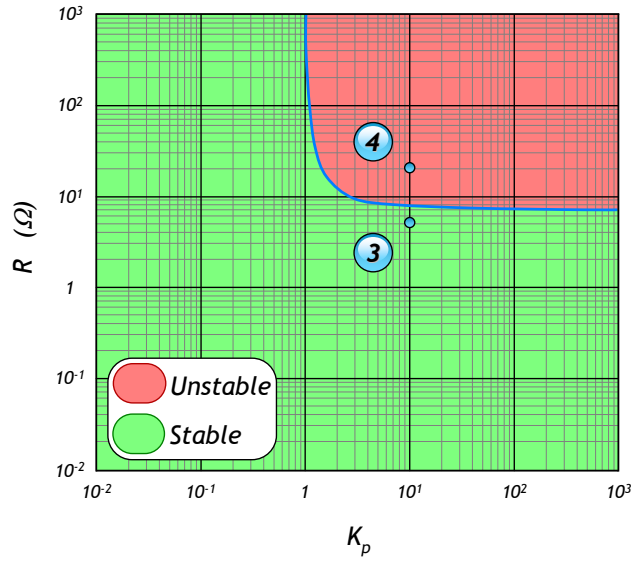

Fig. 14. Stability analysis with a sweep on K_p, R parameters

A similar plot is obtained with two areas separated by the stability limit. To validate those results, simulations for two particular points are also performed (Fig. 15).

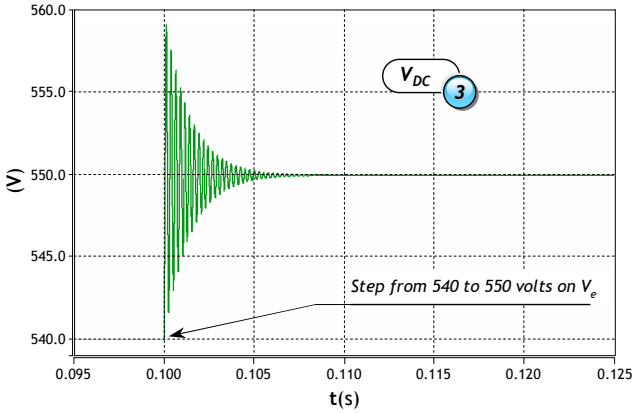

(a) Simulation with the parameters defined in point 3 ($K_p = 10$ and $R = 5\Omega$)

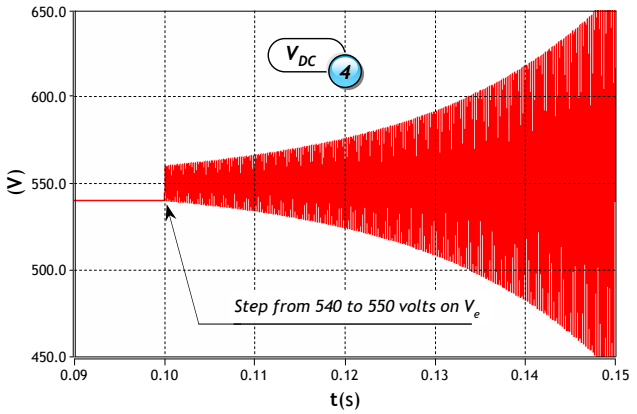

(b) Simulation with the parameters defined in point 4 ($K_p = 10$ and $R = 20\Omega$)

Fig. 15. V_{DC} voltage evolution for different R values

Once again, simulation results (Fig. 15) are in agreement with analysis results.

8 Conclusion

An approach to model electric drive has been presented using the Park frame. The used methods lead to a description of the input admittance of this drive, in the time domain as well as in the frequency one.

In a first step, the model is defined in the time domain: the machine as well as the inverter are described in the Park frame. The obtained (dq) analytical model is implemented on *Saber*. Simulations are performed to validate this model, comparing it with a full model and an

(abc) one.

In a second step, the model is translated in the frequency domain. A linearization around an operating point is applied to reach a transfer function. A Bode diagram validates this averaged model for frequencies below the switching frequency.

Those models are very useful for the stability studies of the drive associated with its input filter. The *Routh-Hurwith* criterion is applied to the transfer function and permits to evaluate the stability, according to the choice of the system's parameters set. Sweeps on filter and regulator parameters are used to qualify the stability of the operating domains.

In a competitive industrial context, these plotted abaci are very useful tools for the designers: they enable to take into account stability criteria from the first beginning of the designer process. In addition, study is analytical during the whole process which can help in parameter studies.

Next step will consist in using this tool to have an overview of interactions between several loads connected to the same DC bus. The same approach will be used: analytical model will allow stability domain specification and time-domain *Saber* model will validate the results.

Appendix: System parameters

The following table contains the parameters values used for stability analysis and simulations.

Element	Unit	Value
R_s	Ω	0.14
L_{dq}	H	$34 \cdot 10^{-6}$
ϕ_M	Wb	0.0226
N_p	$-$	3
J	$kg \cdot m^2$	$730 \cdot 10^{-6}$
f	$N \cdot m \cdot s$	$2.2 \cdot 10^{-3}$
f_{load}	$N \cdot m \cdot s$	$2.2 \cdot 10^{-3}$
P	W	$30 \cdot 10^3$
V_e	V	540
f_s	Hz	1767
f_{sw}	Hz	$20 \cdot 10^3$
Ω_{rated}	$rd \cdot s^{-1}$	3700.8
$T_{em_{rated}}$	Nm	8.106
K_p	$-$	0.46
τ_i	s	$8.53 \cdot 10^{-5}$

Acknowledgment

This research is being conducted in the frame of the MOET project (More-Open Electrical Technologies), a FP6 European Integrated Project [8]. The authors wish to thank the electrical engineering department of Airbus-France for their support.

References

1. J. Liu, X. Feng, F. Lee, and D. Borojevich, "Stability margin monitoring for dc distributed power systems via perturbation approaches," *Power Electronics, IEEE Transactions on*, vol. 18, no. 6, pp. 1254–1261, Nov. 2003.
2. M. Florez-Lizarraga and A. Witulski, "Input filter design for multiple-module dc power systems," in *Power Electronics Specialists Conference, 1993. PESC '93 Record., 24th Annual IEEE*, 20-24 June 1993, pp. 108–114.
3. P. L. Dowell, *Effects of eddy currents in transformer windings.* Proceedings IEE. (UK), August 1966, vol. 113, no. 8.
4. Paice, "Power electronics converters harmonics - multipulse methods for clean power," *IEEE Press*, 1996.
5. R. D. Middlebrook, "Input filter considerations in design and application of switching regulators," *Proc. IEEE Industry Applications Society Annual Meeting*, pp. 366–382, 1976.
6. R. D. Middlebrook and S. Cuk, "A general unified approach to modelling switching-converter power stages," *IEEE Power Electronics Specialists Conference*, vol. 42, pp. 521–550, 1976.
7. A. de Oliveira, J. de A. Monteiro, M. Aguiar, and D. Gonzaga, "Extended dq transformation for vectorial control applications of non-sinusoidal permanent magnet ac machines," in *Power Electronics Specialists Conference, 2005. PESC '05. IEEE 36th*, 2005, pp. 1807–1812.
8. MOET Project, http://www.moetproject.eu.